REPORT DOCUMENTATION PAGE

Form Approved
OMB No. 0704-0188

PLEASE DO NOT RETURN YOUR FORM TO THE ABOVE ADDRESS.

1. REPORT DATE *(DD-MM-YYYY)*	2. REPORT TYPE	3. DATES COVERED *(From - To)*
30-10-2012	Final Technical	03/01/2009-10/31/2012

4. TITLE AND SUBTITLE

Lipid - derived biofuels:Determination of factors that control triacylglyceride accumulation in microalgae

5a. CONTRACT NUMBER

5b. GRANT NUMBER

FA9550-09-1-0243

5c. PROGRAM ELEMENT NUMBER

6. AUTHOR(S)

PI: Cooksey, Keith E

Co-PIs:
Fields, Matthew
Peyton, Brent
Carlson, Ross

5d. PROJECT NUMBER

5e. TASK NUMBER

5f. WORK UNIT NUMBER

7. PERFORMING ORGANIZATION NAME(S) AND ADDRESS(ES)

Montana State University

8. PERFORMING ORGANIZATION REPORT NUMBER

9. SPONSORING/MONITORING AGENCY NAME(S) AND ADDRESS(ES)

AFOSR
875 N. Randolph St
Arlington, VA 22203
Dr. Patrick Bradshaw/RSPE

10. SPONSOR/MONITOR'S ACRONYM(S)

11. SPONSOR/MONITOR'S REPORT NUMBER(S)

AFRL-OSR-VA-TR-2012-1211

12. DISTRIBUTION/AVAILABILITY STATEMENT

Distribution A: Approved for public release; distribution is unlimited

13. SUPPLEMENTARY NOTES

none

14. ABSTRACT

The generality of earlier work with a Chlorophyte was verified in four other Chlorophytes and three diatoms. Neutral lipid droplet accumulation was dependent on medium pH at stationary phase.It was not entirely dependent on medium N and responded positively to bicarbonate addition (25-50mM) to the medium close to stationary phase. Bicarbonate inhibited cell replication in Chlorophytes but not in diatoms, indicating different Inorganic carbon acquisition systems. Effects of N and P limitation were cumulative. Transcriptomic analyses of Phaeodactylum tricornutum cultures when lipid accumulation was maximal showed that genes related to P or N acquisition were up-regulated, as were genes related to carbon uptake (possible C-4 pathway). Expression of genes involved directly in lipid accumulation were unchanged, suggesting that control of lipid accumulation is not at the level of acetyl CoA carboxylase, but earlier in the pathway. Real time PCR supported these conclusions. Changes in expression of genes related to control of the cell cycle (Cyclins) were observed which may explain a general mechanism for lipid accumulation in microalgae

15. SUBJECT TERMS

Bio-jet fuel, microalgae, Chlorophytes, diatoms, bicarbonate, genomic analysis, triacyl glyceride, lipid analysis, pH changes

16. SECURITY CLASSIFICATION OF:			17. LIMITATION OF ABSTRACT	18. NUMBER OF PAGES	19a. NAME OF RESPONSIBLE PERSON
a. REPORT	b. ABSTRACT	c. THIS PAGE			Keith E. Cooksey
unclassified	unclassified	unclassified	unclassified (U)	18	19b. TELEPHONE NUMBER *(Include area code)* 406 - 994 6136

INSTRUCTIONS FOR COMPLETING SF 298

1. REPORT DATE. Full publication date, including day, month, if available. Must cite at least the year and be Year 2000 compliant, e.g. 30-06-1998; xx-06-1998; xx-xx-1998.

2. REPORT TYPE. State the type of report, such as final, technical, interim, memorandum, master's thesis, progress, quarterly, research, special, group study, etc.

3. DATES COVERED. Indicate the time during which the work was performed and the report was written, e.g., Jun 1997 - Jun 1998; 1-10 Jun 1996; May - Nov 1998; Nov 1998.

4. TITLE. Enter title and subtitle with volume number and part number, if applicable. On classified documents, enter the title classification in parentheses.

5a. CONTRACT NUMBER. Enter all contract numbers as they appear in the report, e.g. F33615-86-C-5169.

5b. GRANT NUMBER. Enter all grant numbers as they appear in the report, e.g. AFOSR-82-1234.

5c. PROGRAM ELEMENT NUMBER. Enter all program element numbers as they appear in the report, e.g. 61101A.

5d. PROJECT NUMBER. Enter all project numbers as they appear in the report, e.g. 1F665702D1257; ILIR.

5e. TASK NUMBER. Enter all task numbers as they appear in the report, e.g. 05; RF0330201; T4112.

5f. WORK UNIT NUMBER. Enter all work unit numbers as they appear in the report, e.g. 001; AFAPL30480105.

6. AUTHOR(S). Enter name(s) of person(s) responsible for writing the report, performing the research, or credited with the content of the report. The form of entry is the last name, first name, middle initial, and additional qualifiers separated by commas, e.g. Smith, Richard, J, Jr.

7. PERFORMING ORGANIZATION NAME(S) AND ADDRESS(ES). Self-explanatory.

8. PERFORMING ORGANIZATION REPORT NUMBER. Enter all unique alphanumeric report numbers assigned by the performing organization, e.g. BRL-1234; AFWL-TR-85-4017-Vol-21-PT-2.

9. SPONSORING/MONITORING AGENCY NAME(S) AND ADDRESS(ES). Enter the name and address of the organization(s) financially responsible for and monitoring the work.

10. SPONSOR/MONITOR'S ACRONYM(S). Enter, if available, e.g. BRL, ARDEC, NADC.

11. SPONSOR/MONITOR'S REPORT NUMBER(S). Enter report number as assigned by the sponsoring/ monitoring agency, if available, e.g. BRL-TR-829; -215.

12. DISTRIBUTION/AVAILABILITY STATEMENT. Use agency-mandated availability statements to indicate the public availability or distribution limitations of the report. If additional limitations/ restrictions or special markings are indicated, follow agency authorization procedures, e.g. RD/FRD, PROPIN, ITAR, etc. Include copyright information.

13. SUPPLEMENTARY NOTES. Enter information not included elsewhere such as: prepared in cooperation with; translation of; report supersedes; old edition number, etc.

14. ABSTRACT. A brief (approximately 200 words) factual summary of the most significant information.

15. SUBJECT TERMS. Key words or phrases identifying major concepts in the report.

16. SECURITY CLASSIFICATION. Enter security classification in accordance with security classification regulations, e.g. U, C, S, etc. If this form contains classified information, stamp classification level on the top and bottom of this page.

17. LIMITATION OF ABSTRACT. This block must be completed to assign a distribution limitation to the abstract. Enter UU (Unclassified Unlimited) or SAR (Same as Report). An entry in this block is necessary if the abstract is to be limited.

Lipid-Derived Biofuels: Determination of Factors that Control Triglyceride Accumulation in Microalgae

Principal Investigator
Dr. K.E. Cooksey
Department of Microbiology
109 Lewis Hall
Montana State University
Bozeman, MT 59717
umbkc@ montana.edu; 406-994-6136

Objectives

The objectives of this project were to understand and improve microalgal cellular neutral lipid generation for biofuel production through an examination of the biochemical and molecular processes important in the accumulation of intracellular triacylglycerides (TAGs). The following tasks were proposed in order to address these objectives.

Task 1. Screen green algae and diatom cultures to find the extent to which previously published results can be considered general for microalgae.

Task 2. Quantify growth kinetics and TAG yield parameters for *Phaeodactylum tricornutum* and promising strains passed on from Task 1.

Task 3. Quantify global gene expression to identify metabolic control points governing TAG accumulation in *Phaeodactylum tricornutum.*

Task 4. Develop metabolic flux networks to optimize TAG accumulation in *Phaeodactylum tricornutum.*

The extent to which progress has been made is documented below:

Task 1. Screen suitable green algae and diatoms cultures to find the extent to which previous results can be found to be general for microalgae.

Before this project, detailed information on the effects of environmental parameters and how they interact was generally available for one organism only. This was from our previous work with a Chlorophyte, Chlorella Chor-1. The following: was shown:
(a). Nitrogen limitation (as NO_3^-) was not necessary for cells to accumulate neutral lipid droplets as demonstrated by increases in fluorescence of Nile Red stained cells. It should be pointed out that fluorescence of Nile Red-stained cells has been shown to depict the cellular content of neutral lipid accurately. In most cases, results with Nile Red staining were confirmed by gas chromatographic analyses. For instance, a final Nile Red specific fluorescence

(fluorecsence/cell) reading of 24.8 correlated to 15.2 % TAG based on previous correlation data, $R^2 = 0.95$

$$\%TAG = (\text{Nile Red specific fluorescence} - 1.104)1.56^{-1}$$

(b). Unless the pH of the medium was allowed to rise as result of photosynthesis, no TAG was accumulated. The critical pH value needed to be achieved is of the order of pH 10.5.

(c). Addition of 5mM $NaHCO_3$ near the stationary phase of growth stalled the cell cycle and caused an immediate cessation of cellular growth and an increase in TAG accumulation.

Seven cultures of microalgae (four Chlorophytes and three diatoms) were tested. There were some changes in how the experiments were performed. In the former works experiments 24 hr illumination (75 micromoles/$m^{2/}$sec) was used and 100mL cultures were shaken. In the work reported here cells were grow in 1.25L bioreactors (Fig 1) illuminated (400 µmole.m^{-2}·s^{-1} photon flux) with a 14 hr light/ 10hr dark schedule. Further, this design allowed aeration with various gas mixtures. All seven responded similarly to Chlorella, i.e., if the medium pH was allowed to increase, the Nile Red signal was considerably enhanced and obtained its maximal value much more quickly.

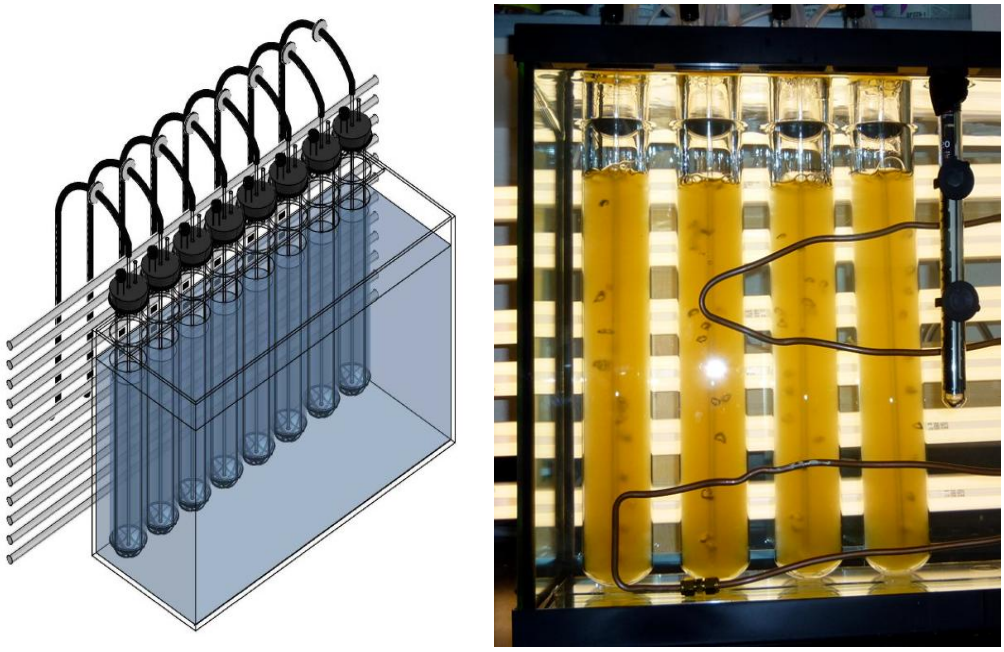

Figure 1 – Aeration, temperature, and light-controlled 1.25 L vertical airlift photobioreactors which were designed specifically for this project to increase biomass production and greater freedom of sampling. Cells shown growing here are *Phaeodactylum tricornutum.*

Table 1 summarizes the results obtained with six of these cultures. Two of the diatom cultures (Pt1 and Pt 642) were obtained from culture collections. RGd -1 was isolated from an alkaline spring in Yellowstone National Park as was Scenedesmus sp. WC-1. Chlorophyte EN 00002 was provided by AFOSR grantee Juegen Polle and Chlamydomonas CC 124 came from Matthew Posewitz at CO School of Mines. All cells except Pt642 responded to bicarbonate addition with a

rapid increase in the Nile Red fluorescence signal. Pt642 responded similarly to the other cells if vanadate was added to the culture. Vanadate is an ATP-ase inhibitor. Currently we have no metabolic explanation for its effect on TAG accumulation. Bicarbonate generally reduced the time to maximal TAG accumulation and increased the maximal yield of this material several fold. It is obvious that inorganic carbon acquisition differs between diatoms and green algae as diatoms continued to grow for at least 1-2 generations, whereas green microalgae stopped growing as soon as bicarbonate was added. Bicarbonate is therefore not merely a source of inorganic carbon, but has other actions and these differ between greens and diatoms. It is our conclusion that our results obtained previously with Chlorella are probably general for microalgae, although diatoms and green algae differ in their response to added bicarbonate.

Table 1 Influence of bicarbonate addition on TAG accumulation in a selection of microalgae.

Organism	$NaHCO_3$ addition	Time to peak TAG, HCO_3/control (days)	Peak TAG v. control, fold increase	Growth continues after HCO_3addition?
Pt1: diatom	**25mM**	**5.5/6.0**	**8.1**	**yes**
Pt 642: diatom	**25mM**	**5.6/6.0 Van***	**3.2**	**yes**
RGd-1: diatom	**25mM**	**10/16**	**1.6**	**yes**
WC-1: green	**50mM**	**8/16**	**9.7**	**no**
EN 0002: green	**50mM**	**9/11**	**No difference**	**no**
Chlamydomonas sp.: green	**50mM**	**6/6**	**4.6**	**no**

*** Vanadate added**

Task 2) Quantify growth kinetics and TAG yield parameters for *Phaeodactylum tricornutum* and promising strains passed on from Task 1

Phaeodactylum tricornutum 1055/1, also referred to here as Pt1, was acquired from the Provasoli-Guillard National Center for Culture of Marine Phytoplankton (CCMP 2561) (West Boothbay Harbor, Maine). This organisms was chosen for transcriptomic and other genetic investigations because its full genome has been sequenced. The diatom grows on ASP2- a marine artificial medium and maintains the fusiform morphology when the medium Ca^{++} is maintained at 5mM which is 2x its usual concentration. In addition, based on the screening done in Task 1, *WC-1* was determined to be a promising fuel production strain. Growth/TAG accumulation optimization experiments were performed using these algae. The main objective of this work was to enhance TAG accumulation per cell while at the same time maintaining or increasing biomass production.

Variables chosen for study included the use of ambient air alone or 5% CO_2 in air and the addition of sodium bicarbonate to the medium. This addition was made before or after nitrate in the growth medium was depleted. CO_2 enriched air caused the pH to be reduced below the optimal level in Phaeodactylum and TAG accumulation was lessened. Scenedesmus WC-1 behaved similarly, but as has been mentioned earlier, cell replication was stalled on addition of bicarbonate to the medium. The lowering of pH when 5% CO_2 was used can be explained by its non-use during dark periods and in the light when N was depleted. The timing of bicarbonate

addition proved to be critical. If added after nitrate in the medium was exhausted, no increase in TAG accumulation over controls was observed. These results are provided in detail in Table 2.

Table 2: Growth and lipid production properties of *Scenedesmus* sp.*WC-1* and *P. tricornutum* cultured in unbuffered Bold's basal and ASP2 media, respectively, during 14:10 light-dark cycling (n=3).

Organism	Aeration	Time of HCO_3 Addition (d)	Time of Harvest (d)	Final Cell Density ($x10^7$ cells mL^{-1})	Dry Weight (g/L) (DCW)[a]	Final Total Nile Red Fluorescence ($x10^3$ units)	Final Specific Nile Red Intensity $Cell^{-1}$ [b]
Scenedesmus WC-1	Air	N/A	18.0	2.46 ± 0.06	1.1 ± 0.1	36.8 ± 5.2	15.0 ± 2.3
	5% CO_2	N/A	14.0	5.87 ± 0.15	2.7 ± 0.1	1.2 ± 0.2	0.2 ± 0.1
	5% CO_2 → Air	N/A	8.0	2.69 ± 0.69	0.8 ± 0.1	1.0 ± 0.4	0.4 ± 0.1
	5% CO_2 → Air	3.7 [c]	8.0	1.34 ± 0.15	1.1 ± 0.1	33.5 ± 6.3	24.8 ± 2.2
	5% CO_2 → Air	6.4 [d]	12.0	5.18 ± 0.41	2.1 ± 0.0	0.3 ± 0.3	0.1 ± 0.1
Phaeodactylum Pt-1	Air	N/A	9.0	1.17 ± 0.04	0.2 ± 0.0	0.6 ± 0.4	0.3 ± 0.2
	Air	3.0 [c]	5.0	0.65 ± 0.01	0.1 ± 0.0	6.5 ± 0.9	9.9 ± 0.8
	Air	7.0 [d]	9.0	1.02 ± 0.05	0.1 ± 0.0	0.1 ± 0.1	0.1 ± 0.1

[a] Dry cell weight (DCW) determined gravimetrically with filtered samples dried at 60°C
[b] Calculated by fluorescence signal/cell density x 10,000 (scaling factor)
[c] Pre-nitrate depletion
[d] Post-nitrate depletion
N/A – not applicable

Points notable inTable 2 :
(a). WC-1 grew to a greater density(x2.5) with 5% CO_2 supplemented air than with air alone , but the TAG accumulation (Nile Red fluorescence/cell) was 75x greater with unsupplemented air.
(b).The influence of the timing of the addition of bicarbonate was shown to be critical (250 fold difference) in the specific fluorescence/cell (Column 8).
(c). *Phaeodactylum* showed that the fluorescence/cell was 100 x higher if bicarbonate was added before total depletion of nitrate.

To elucidate *P. tricornutum* gene expression profiles during nutrient-deprivation and lipid-accumulation it was essential to understand the effects of various levels of nutrient limitation. Cultures were grown with a nitrate to phosphate ratio of 20:1 (N:P) and whole-genome transcripts were monitored over time via RNA-sequence determination. The specific Nile Red (NR) fluorescence (NR fluorescence per cell) increased over time; however, the increase in NR fluorescence was initiated before external nitrate was completely exhausted. Exogenous phosphate was depleted before nitrate, and these results indicated that the depletion of exogenous phosphate might be an early trigger for lipid accumulation that is magnified upon nitrate depletion.
Nitrogen and phosphorus limitation can initiate the stationary phase of growth and induce lipid accumulation independently, as well as in a complementary manner. Maintaining replete

nitrogen and phosphorus (NO_3^- and PO_4^-) conditions in the medium maintained a higher dissolved inorganic carbon (DIC) requirement in the system and slowed growth, but did not cause cells to accumulate lipid. This suggests that nutrient stress, particularly NO_3^- and PO_4^- are necessary for cells to accumulate lipid. Under nutrient deplete conditions of NO_3^-, PO_4^- or both ions, *P. tricornutum* accumulated lipids. In order to determine if this metabolic shift was reversible, each condition was supplemented with NO_3^-, PO_4^- or both. Thus, in cells that were NO_3^- deplete but PO_4- replete, the supplementation of NO_3^- caused cells to reverse lipid accumulation. The same effect was observed for cells that were PO_4^{3-} deplete but NO_3^- replete, the supplementation of PO_4^{3-} caused cells to reverse lipid accumulation. In addition, lipid accumulation was reversed when both nutrients were added back to the medium. The results showed a shift from lipid accumulation to its catabolism in all three conditions (NO_3^-, PO_4^{3-} or both). Cell numbers slightly increased signifying a metabolic shift from storage or lipid accumulation to growth and energy consumption. This result shows that lipid accumulation is reversible as cells maintained a dynamic state to shift away from accumulation and back to growth. During exponential nutrient replete growth we observed a large consumption of DIC to the point that DIC became limiting but not deplete. As fatty acid synthesis consumes bicarbonate , increased DIC levels were tested and correlated with increased lipid accumulation. When the CO_2 concentrations were increased from ambient air to 1% CO_2 in air the DIC remained at an elevated level (>90mg/L DIC for 1% CO_2 compared to 16mg/L DIC of ambient air at equilibrium) so that limitation was not observed. Elevated levels of CO_2 during growth in a nutrient deplete state did not affect growth or increase lipid accumulation. Thus, increased DIC throughout growth does not correlate to increased lipid content nor does it need to be limited to initiate lipid accumulation. Lipid accumulation analysis was carried out using the Nile red fluorescence assay. Confirmation of the Nile Red results was done by the analysis of fatty acid methyl esters (FAMEs) using gas chromatography/mass spectrometry. Profiles of FAMEs remained similar but significant abundance differences were seen which depended on the replete or deplete condition of the cells, confirming the Nile red assay results. This work supports the hypothesis that TAG accumulation occurs only when the cell cycle is stalled by the lack of essential nutrients (or subject to other stresses, such as the pH of the medium).

The work described so far has involved has not involved a Chlorophyte that may be used industrially to provide precursors for the production of bio-jet fuel. Thus *Chlamydomonas reinhardtii* was selected for the same type of studies already performed. The ability to make modifications to its genome makes *Chlamydomonas* a strong contender for industrial exploitation. Thus a comprehensive investigation into inorganic carbon source (high and low CO_2 along with high bicarbonate) during TAG and starch accumulation was done on with this organism. *C. reinhardtii* utilizes ammonium as its N-source so that this provides further insight into mechanisms whereby nutrient levels control TAG accumulation.

C. reinhardtii grew rapidly with 5% CO_2 in air until ammonium in the medium was depleted. During this time there was a characteristic decrease in pH, which is usual when microalgal are grown on ammonium and at a high CO_2 level. During ammonium depletion, *C. reinhardtii* accumulated TAG and starch as carbon storage compounds when either 5% CO_2 aeration or bicarbonate was used as an inorganic carbon source. After ammonium depletion, the 5% CO_2 aerated cultures accumulated starch quickly which then fell in concentration. It is possible that the starch was then reallocated to TAG. The highest TAG accumulation was observed when cultures were aerated with 5% CO_2 in air. Fatty acid methyl ester analyses using

in situ methylation indicated that the TAG began to degrade into free fatty acids and diacylglycerol within a few days. While the 50 mM bicarbonate amended cultures accumulated starch and TAG at a slightly slower rate, starch reallocation and stable carbon storage was observed. The cultures grown using air alone exhibited carbon limitation and slow metabolic growth with minimal TAG or starch accumulation.

The highest biofuel potential in Chlamydomonas cultures was observed when high CO_2 in air was used as the carbon substrate. However, these conditions were not as stable, in comparison with bicarbonate as the inorganic carbon source, as evidenced by the fast accumulation followed by somewhat rapid degradation of both TAG and starch. Additionally the bicarbonate amended cultures exhibited more carbon storage, due to the high starch remaining at the end of the experiments. This suggests industrial use of algae to produce biofuel could benefit from using bicarbonate during nutrient deplete conditions to boost output, especially if the industrial strain does not have the capabilities to produce starch, such as *C. reinhardtii* starchless mutants.

Task 3. Transcriptomic Analysis of Lipid Accumulation in *Phaeodactylum tricornutum*

The full genome of *Phaeodactylum tricornutum* has been sequenced (<30 Mb), and approximately 20 to 30% triacylglyceride (TAG) accumulation on a dry cell basis has been reported under different growth conditions. This organism was therefore ideal for the analyses proposed. To elucidate *P. tricornutum* gene expression profiles during nutrient-deprivation and lipid-accumulation, cell cultures were grown with a nitrate to phosphate ratio of 20:1 (N:P) and whole-genome transcripts were monitored over time using RNA-sequence determination. TAG accumulation was initiated before external nitrate was completely exhausted. Exogenous phosphate was depleted before nitrate, and these results indicated that the depletion of exogenous phosphate might be an early trigger for lipid accumulation that is magnified upon nitrate depletion. As expected, many of the genes associated with nitrate and phosphate utilization were up-expressed. The diatom-specific cyclins *cyc*7 and *cyc*10 were down-expressed during the nutrient-deplete state, and cyclin B1 was up-expressed during lipid-accumulation after growth cessation. While many of the genes associated with the C3 pathway for photosynthetic carbon reduction were not significantly altered, genes involved in a putative C4 pathway for photosynthetic carbon assimilation were up-expressed as the cells depleted nitrate, phosphate, and exogenous dissolved inorganic carbon (DIC) levels. *P. tricornutum* has multiple, putative carbonic anhydrases, but only two were significantly up-expressed (2-fold and 4-fold) at the last time point when exogenous DIC levels had increased after the cessation of growth. Alternative pathways that could utilize HCO_3^- were also suggested by the gene expression profiles (*e.g.*, propionyl-CoA, methylmalonyl-CoA, putative decarboxylase). Overall, the results indicate that *P. tricornutum* continued carbon dioxide reduction when population growth was arrested and different carbon-concentrating mechanisms were used dependent upon exogenous DIC levels. Based upon overall low gene expression levels for fatty acid synthesis, the results also suggest that the build-up of precursors to the acetyl-CoA carboxylases may play a more significant flux toward TAG synthesis rather than the enzyme levels of acetyl-CoA carboxylases *per se*. These results suggest that carbon is being "pushed" into fatty acid synthesis via elevated acetyl-CoA and NADPH levels and thus not being "pulled" by a large abundance of fatty acid synthesis activity. With respect to lipid accumulation, we hypothesize that the "hinge" is the committed step in fatty acid biosynthesis (*i.e.*, acetyl-CoA carboxylase), but that a "push" condition

accounts for a significant portion of the metabolic flux based upon gene expression. The insights into the types and timing of cellular responses to inorganic carbon presented will help maximize photoautotrophic carbon flow to lipid accumulation.

Task 4. Develop metabolic flux networks to optimize TAG accumulation in *Phaeodactylum tricornutum*.

Molecular-level data on more than 50 central metabolism transcripts were measured using Real Time PCR. Analysis of transcripts suggested that the central metabolism pathways associated with bicarbonate transport, carbonic anhydrases, and C-4 carbon fixation were important for lipid accumulation. Transcriptomic data also suggested that repurposing of phospholipids may play a role in lipid accumulation. This study provides a detailed physiological and molecular-level foundation for improved understanding of diatom nutrient cycling and contributes to a metabolic blueprint for understanding and controlling lipid accumulation in diatoms.

An *in silico* metabolic model of the diatom *P. tricornutum* was built from genome data, transcriptomic data and literature reviews. The metabolic model accounts for 680 genes from the nuclear and chloroplastic genomes integrated into 319 enzyme catalyzed reactions, many reactions account for multiple gene products (see Appendix for listing of reactions). The enzymes and metabolites are all partitioned into 5 subcellular compartments (cytosol, mitochondrion, peroxisome, plastid, extracellular space) to explore the role of compartmentalization on metabolic function. The model enzymes were correlated with a previously published RNA-seq analysis of this diatom to include all enzymes which had significant changes in transcript (see Task 3). Cellular biomass synthesis was considered using a literature review of diatom macromolecular content as well as vitamin and trace mineral content. The computational model has been solved for all possible pseudo-steady state solutions using both convex basis analysis using CellNetAnalyzer and elementary flux modes using efmtool. 145,761 convex basis vectors were identified while approximately one billion elementary flux modes were enumerated. Mathematically the elementary flux modes can be defined using combinations of convex basis vectors so the analysis has focused initially on the more manageable convex basis vectors; however, a comparison of the two data sets will provide an informed basis for the necessity of calculating both aspects of metabolic networks. The ongoing analysis has explicitly defined the relationship between the numerous genome encoded C-3 and C-4 carboxylases enzymes and the efficiency of synthesizing biomass during growth and the synthesis of triacylglycerides under non growth conditions. The analysis focused on combinations of the enzymatic investment requirements such as enzyme nitrogen content to realize a metabolic pathway and the resulting efficiency of the pathway to produce either biomass or TAG. Questions regarding the nutrient investment required for constructing an organelle and how that cost relates to pathway competitiveness remain subjects of going research.

Executive Summary

(a). Research Summary and some conclusions

This report reflects the highlights of published work, manuscripts submitted and projects started under AFOSR auspices, but continued with other support. It was shown that all microalgae studied behave similarly with respect to the conditions necessary to achieve significant triacylglyceride accumulation –the major precursor for bio-jet fuel production. These conditions

can be summarized as follows: the culture must reach a pH level where most of the inorganic carbon in the medium is available as bicarbonate and the cell cycle must be stalled. Stalling the cell cycle is most easily achieved by limiting the concentration of one or more essential nutrients, such as N or P. This information can be used industrially as algae can be grown in nitrogen (as NO_3^- or NH_4^+)and/or phosphorus (as PO_4^{3-})replete media until a high biomass is available when sodium bicarbonate (not sodium carbonate or sodium chloride) can be added as a TAG trigger. All the algae studied responded to bicarbonate in this manner. Nevertheless, it is recommended that industrial algae growers perform studies of the type reported here with organism they intend to use. Although the organisms studied here behaved in a very similar fashion to one another, their physiological responses to manipulation of the growth conditions were *not* identical. Differences between Chlorophytes and diatoms, especially in their responses to added bicarbonate were obvious. Carbon concentrating mechanism (CCM) of microalgae are well known but the information available is limited to concentrating of bicarbonate similar to that in sea water, i.e.,15- 25 fold less that was used in this study. It is highly likely that the influence of added bicarbonate at environmental levels (2mM) will not be the same as that added at 30-50mM. The CCM in green microalgae involves carbonic anhydrase whereas that in diatoms does not. Diatoms can transport and utilize bicarbonate by converting it to malate (a C-4 acid) as an intermediate. It is proposed that the 15-25 fold increase in the bicarbonate ion inhibits the enyzyme(s) necessary for its utilization in green algae as a source of inorganic carbon for growth, leaving fatty acids as the only sink. Diatoms, as has been shown here, can use a C-4 pathway involving pyruvate carboxylase to form malate and the malic enzyme to regenerate CO_2 at the chloroplast. These ideas have been the basis of three invited lectures.

(b). Persons involved in the work reported here

Students

Graduate Students
Robert Gardner (now has PhD)
Jacob Valenzuela
Karen Moll
Egan Lohman
Everett Eustace

Undergraduates
Patrizia Peters, Visiting student from Germany
Jean – Paul Toussaint.

Post Doctoral Fellows
Florence Mus

Faculty
Brent Peyton, MSU
Matthew Fields, MSU
Ross Carlson, MSU
Robin Gerlach,MSU
Richard Macur,MSU
Aurelien Mazurie,MSU

Gregory Helms, Washington State University
William Hiscox, Washinton State University
Rose-Ann Cattolico, University of Washington
John Beardall, Monash University, Australia
Keith Cooksey, MSU

(c). Manuscripts accepted and published as a result of AFOSR funding

Robert Gardner, Patrizia Peters, Brent Peyton, Keith Cooksey. (2011) Medium pH and Nitrate concentrration Effects on Accumulation of Triacylglycerol in Two Members of the Chlorophyta. Journal of Applied Phycology 23(6): 1005-1016.

Robert D. Gardner, Keith E. Cooksey, Florence Mus, Richard Macur, Karen Moll, Everett Eustance, Ross Carlson, Robin Gerlach, Matthew Fields, Brent M. Peyton. (2012a) Use of Sodium Bicarbonate to Stimulate Triacylglycerol Accumulation in the Chlorophyte *Scenedesmus* sp. and the Diatom *Phaeodactylum triconutum*. Journal of Applied Phycology 24(5): 1311-1320.

Robert D. Gardner, Egan Lohman, Robin Gerlach, Keith E. Cooksey, Brent M. Peyton. (2012b) Comparison of CO_2 and Bicarbonate as Inorganic Carbon Sources for Triacylglycerol and Starch Accumulation in *Chlamydomonas reinhardtii*. Biotechnology and Bioengineering DOI 10.1002/bit.24592.

Robert D. Gardner, Egan Lohman, Robin Gerlach, Keith E. Cooksey, Brent M. Peyton. (2012c) CO_2 or Bicarbonate for Algal Lipid Production. Spotlight feature for Biotechnology and Bioengineering (solicited, in press)

Gardner RD. 2012. Control of Triacylglycerol Accumulation and Bicarbonate-Induced Accumulation in Microalgae [Dissertation]. Bozeman, MT: Montana State University. 164 p. http://search.proquest.com/docview/1046459772

Valenzuela, J., A. Mazurie, R. Carlson, R. Gerlach, K.E. Cooksey, B.M. Peyton, and M.W. Fields. 2012. Potential role of multiple carbon fixation pathways during lipid accumulation in *Phaeodactylum tricornutum*. Biotechnol. Biofuels 5:40. http://www.biotechnologyforbiofuels.com/content/5/1/40

Standards Committee of the Algae Biomass Organization, Co- chair K.E. Cooksey. Existing and proposed standards pertinent to the algae industry. http://algaebiomass.org/ policy center/ technical standards.

(d). Submitted Manuscripts

Mus, F., Toussaint,J.-P., Cooksey, K.E., Gerlach,R, .Fields, M., Peyton, B. and Carlson, R. 2012 Physiological and molecular analysis of carbon source supplementation and pH stress-induced accumulation of lipid accumulation in the marine diatom *Phaeodactylum tricornutum*. Appl Microbiol and Cell Physiol: submitted.

Patents

US Patent Application number 61/386,260 "Bicarbonate trigger for inducing lipid accumulation in algal systems", Submitted September 24th, 2010. Inventors: K. E. Cooksey, R. D. Gardner, B. M. Peyton.

PCT International Patent Application No: PCT/US2011/053238 "Bicarbonate trigger for inducing lipid accumulation in algal systems", Filed September 26th, 2011. Inventors: K. E. Cooksey, R. D. Gardner, B. M. Peyton.

Projects started under AFOSR auspices but continued with other funding.

(a).Analytical standard methods for algal products

A collaborative project has been initiated between Montana State University, the National Renewable Energy Lab (Lieve Laurens), and the University of Washington (Rose Ann Cattolico) It is aimed at evaluating/refining biofuel analysis methods. *Chlorella* sp/ biomass supplied to MSU and UW from NREL was then analyzed at all three institutions to evaluate institutional variability and method variability. Results are shown in Table 2. Method MSU/ Griffith provided the most consistent information.

Table 2- Direct transesterification results on Chlorella sp. biomass which was analyzed at Montana State University, National Renewable Energy Lab, and University of Washington (n=3).

Institution	Biomass Analyzed	Method	FAME Content (%DCW±SD)
MSU	31-38 mg	Griffith	12.26 ± 0.08
MSU	1.5-9 mg	SUMI	11.71 ± 0.48
UW	0.8-1.1 mg	SUMI	7.36 ± 1.32
NREL		NREL	9.78

(b).NMR study of the utilization ^{13}C- sodium bicarbonate as a triacylglyceride accumulation trigger in *Chlorella* sp. Gardner, R., Cooksey, KE (both MSU), and Gregory Helms and William Hiscox, both from Washington State University. This project is focused on using high resolution – magic angle spinning (HR-MAS) and static NMR to monitor the accumulation of biofuel precursors in a *Chlorella* sp.. Further, $H^{13}CO_3^-$ uptake is being investigated using NMR to determine the amount of bicarbonate incorporated into TAG during bicarbonate additions. Preliminary results show a strong correlation between NMR and the sum of free fatty acids, mono-, di-, and triacylglycerols determined by gas chromatography.

(c). Systems Biology approach to understanding nutrient deprived lipid accumulation during the diel cycle of *Phaeodactylum tricornutum*, Fields, M. and Valenzuela, J.(both MSU).

Most instances where lipid accumulation occurs is monitored during the light cycle. However, lipid yield is the sum of what is accumulated minus what is consumed. Therefore, understanding metabolic control points during light and dark periods may provide improved insight into carbon flow due to large differences in reducing equivalents (active vs. non-active photosystems). In order to investigate these control points we will take a systems biology approach utilizing transcriptomics, proteomics, and metabolomics. Expression data is very valuable when approaching metabolism from a whole cell standpoint, but complementing it with proteomics can resolve physiological tendencies with greater discretion. Proteomics takes snapshots of the phenotype of an organism, i.e. what exactly is being expressed and functionally dictating cellular physiology. If proteomics is the phenotypic expression of gene functionality, the metabolites are the sum of the substrates and products dictated by the physiological phenotype. To compliment both gene transcripts and expression, the analyses will be completed with metabolomics. Metabolomics offers a look into the possible metabolic fluxes associated with the physiological state of the cell. Metabolite identification and quantification has been initiated and optimization of the extractions and identification parameters are underway. The comprehensive systems biology approach will provide valuable insights into metabolic fluxes driving lipid accumulation during diel cycle growth of *Phaeodactylum tricornutum*.

(d). Ecophysiology and biochemistry of algae , Gardner, R.,Cooksey K. Beardall, J.

A collaborative project has been initiated between Montana State University and John Beardall's laboratory at Monash University in Australia. Prof. John Beardall's laboratory focuses primarily on algal Carbon Concentrating Mechanisms(CCM). The objective of this study was to determine whether CCMs are induced after bicarbonate addition and to elucidate involvement of these CCMs during TAG accumulation. Metabolic inhibitors were used in concert with Nile Red fluorescence of treated cells with and without bicarbonate addition. TAG accumulation was monitored while enzymes involved in lipid metabolism were inhibited specifically. Both *Chlamydomonas reinhardtii* and *Phaeodactylum tricornutum* strain 642 were tested. The metabolic inhibitors used were acetazolamide (AZ) and ethoxyzolamide (EZ), both at 50 µM, to inhibit carbonic anhydrase enzyme function. AZ is specific to extracellular carbonic anhydrases while EZ inhibits both extra- and intracellular carbonic anhydrases. Thus, differentation can be made concerning the influence these carbonic anhydrases have on TAG accumulation. Vanadate (VAN), as sodium orthovanadate (150 – 180 µM) inhibits HCO_3^- /ATPase transport enzymes. Conversely, 4,4'-di-isothiocyanostil-bene-2,2'-disulphonic acid (DIDS) (200 µM) inhibits HCO_3^- anion exchange enzymes. Salicylhydroxamic acid (SHAM) (3 mM), inhibits active CO_2 uptake. The experimental concentrations of inhibitors were taken from the literature.

Nile Red specific fluorescence of *C. reinhardtii* was measured after medium nitrate depletion had taken place. The control cultures (no bicarbonate added) accumulated less than half of the TAG per 10,000 cells when bicarbonate was added. Forty three hours after N depletion the inhibitors AZ, EZ, VAN, and SHAM showed less TAG content than cultures to which only bicarbonate had been added. However after 68 hr post N depleteion, AZ, EZ and VAN showed no significant differences from the bicarbonate control. Cultures to which the DIDS (bicarbonate ion exchange inhibitor) was added, accumulated more TAG than controls. Further analyses are being conducted to determine the implication of these results, but so far they show

that there was no significant effect of these inhibitors that could be explained by their known biochemical activity.

Appendices:

Task 4

Appendix: *Phaeodactylum tricornutum* metabolic model input file.

Reaction 1: C1 : NAD+_c + glycolate_c ==> NADH_c + glyoxylate_c + H+_c
Reaction 2: C2 : ATP_c + GMP_c ==> ADP_c + GDP_c
Reaction 3: C3 : glyoxylate_c + L-glutamate ==> glycine + 2-oxoglutarate_c
Reaction 4: C4 : NADH_c + nitrate_c + H+_c ==> H2O + NAD+_c + nitrite_c
Reaction 5: C5 : 2-oxoglutarate_c + ammonia_c + NADPH_c + 2 H+_c ==> H2O + L-glutamate + NADP+_c
Reaction 6: C6 : H2O + glycine + 5,10-methylenetetrahydrofolate_c <==> tetrahydrofolate_c + L-serine
Reaction 7: C7 : NAD+_c + 5-methyl-tetrahydrofolate_c <==> NADH_c + H+_c + 5,10-methylenetetrahydrofolate_c
Reaction 8: C8 : NADP+_c + 5,10-methylenetetrahydrofolate_c <==> NADPH_c + 5,10-methenyltetrahydrofolate_c
Reaction 9: C9 : 5-formyl-tetrahydrofolate_c + ATP_c <==> 5,10-methenyltetrahydrofolate_c + ADP_c + phosphate_c
Reaction 10: C10 : NAD+_c + formate_c ==> NADH_c + CO2_c
Reaction 11: C11 : tetrahydrofolate_c + ATP_c + formate_c <==> ADP_c + phosphate_c + 10-formyl-tetrahydrofolate_c
Reaction 12: C12 : H2O + 5,10-methenyltetrahydrofolate_c <==> H+_c + 10-formyl-tetrahydrofolate_c
Reaction 13: C13 : H2O + CO2_c <==> H+_c + bicarbonate_c
Reaction 14: C14 : bicarbonate_c + ATP_c + propanoyl-CoA_c ==> H+_c + ADP_c + phosphate_c + (S)-methylmalonyl-CoA_c
Reaction 15: C15 : NAD+_c + phosphate_c + D-glyceraldehyde-3-phosphate_c <==> NADH_c + H+_c + 1,3-diphosphateglycerate_c
Reaction 16: C16 : ATP_c + 3-phospho-D-glycerate_c <==> ADP_c + 1,3-diphosphateglycerate_c
Reaction 17: C17 : ATP_c + D-fructose-6-phosphate_c ==> H+_c + ADP_c + fructose-1,6-bisphosphate_c
Reaction 18: C18 : H2O + fructose-1,6-bisphosphate_c ==> phosphate_c + D-fructose-6-phosphate_c
Reaction 19: C19 : fructose-1,6-bisphosphate_c <==> D-glyceraldehyde-3-phosphate_c + dihydroxyacetone-phosphate_c
Reaction 20: C20 : D-glyceraldehyde-3-phosphate_c <==> dihydroxyacetone-phosphate_c
Reaction 21: C21 : a-D-glucose-1-phosphate_c <==> a-D-glucose-6-phosphate_c
Reaction 22: C22 : a-D-glucose-6-phosphate_c <==> D-fructose-6-phosphate_c
Reaction 23: C23 : H2O + ATP_c + a-D-glucose-1-phosphate_c ==> H+_c + ADP_c + 2 phosphate_c + chrysolaminaran
Reaction 24: C24 : H+_c + ADP_c + phosphoenolpyruvate_c ==> pyruvate_c + ATP_c
Reaction 25: C25 : H2O + NAD+_c + acetaldehyde_c <==> NADH_c + 2 H+_c + acetate_c
Reaction 26: C26 : NAD+_c + ethanol_c <==> NADH_c + H+_c + acetaldehyde_c
Reaction 27: C27 : ATP_c + acetate_c + coenzymeA_c ==> acetyl-CoA_c + diphosphate_c + AMP_c
Reaction 28: C28 : ATP_c + coenzymeA_c + citrate_c ==> ADP_c + phosphate_c + oxaloacetate_c + acetyl-CoA_c
Reaction 29: C29 : 2 acetyl-CoA_c ==> coenzymeA_c + acetoacetyl-CoA_c
Reaction 30: C30 : a-D-glucose-1-phosphate_c ==> a-D-galactose-1-phosphate_c
Reaction 31: C31 : coenzymeA_c + succinate_c + GTP_c ==> phosphate_c + GDP_c + succinyl-CoA_c
Reaction 32: C32 : H2O + CO2_c + phosphoenolpyruvate_c ==> H+_c + phosphate_c + oxaloacetate_c
Reaction 33: C33 : pyruvate_c + L-glutamate ==> L-alanine + 2-oxoglutarate_c
Reaction 34: C34 : NADP+_c + a-D-glucose-6-phosphate_c ==> NADPH_c + H+_c + 6-phospho-D-glucono-1,5-lactone_c
Reaction 35: C35 : H2O + 6-phospho-D-glucono-1,5-lactone_c ==> H+_c + 6-phospho-D-gluconate_c
Reaction 36: C36 : NADP+_c + 6-phospho-D-gluconate_c ==> NADPH_c + CO2_c + D-ribulose-5-phosphate_c
Reaction 37: C37 : D-ribulose-5-phosphate_c <==> D-xylulose-5-phosphate_c
Reaction 38: C38 : D-glyceraldehyde-3-phosphate_c + D-sedoheptulose-7-phosphate_c <==> D-xylulose-5-phosphate_c + D-ribose-5-phosphate_c
Reaction 39: C39 : D-glyceraldehyde-3-phosphate_c + D-sedoheptulose-7-phosphate_c <==> D-fructose-6-phosphate_c + D-erythrose-4-phosphate_c
Reaction 40: C40 : D-xylulose-5-phosphate_c + D-erythrose-4-phosphate_c <==> D-glyceraldehyde-3-phosphate_c + D-fructose-6-phosphate_c
Reaction 41: C41 : ATP_c + D-ribose-5-phosphate_c ==> H+_c + AMP_c + 5-phospho-a-D-ribose-1-diphosphate_c
Reaction 42: C42 : 3 H2O + 2 NAD+_c + ATP_c + L-glutamine + 5-phospho-a-D-ribose-1-diphosphate_c ==> 2 NADH_c + 2-oxoglutarate_c + 5 H+_c + phosphate_c + 2 diphosphate_c + L-histidine + aminoimidazole-carboxamide-ribonucleotide_c
Reaction 43: C43 : 2 H2O + glycine + CO2_c + 4 ATP_c + 10-formyl-tetrahydrofolate_c + 2 L-glutamine + 5-phospho-a-D-ribose-1-diphosphate_c + L-aspartate ==> 2 L-glutamate + 7 H+_c + tetrahydrofolate_c + 4 ADP_c + 4 phosphate_c + diphosphate_c + fumarate_c + aminoimidazole-carboxamide-ribonucleotide_c
Reaction 44: C44 : 10-formyl-tetrahydrofolate_c + aminoimidazole-carboxamide-ribonucleotide_c ==> H2O + tetrahydrofolate_c + inosine-5'-phosphate_c
Reaction 45: C45 : ATP_c + GTP_c + L-aspartate + inosine-5'-phosphate_c ==> 2 H+_c + 2 ADP_c + phosphate_c + fumarate_c + GDP_c
Reaction 46: C46 : ATP_c + redthioredoxin_c ==> H2O + dATP_c + oxthioredoxin_c
Reaction 47: C47 : ATP_c + AMP_c ==> 2 ADP_c
Reaction 48: C48 : 2 H2O + NAD+_c + ATP_c + L-glutamine + inosine-5'-phosphate_c ==> NADH_c + L-glutamate + 3 H+_c + diphosphate_c + AMP_c + GMP_c
Reaction 49: C49 : ATP_c + GDP_c + redthioredoxin_c ==> H2O + ADP_c + dGTP_c + oxthioredoxin_c
Reaction 50: C50 : ATP_c + GDP_c ==> ADP_c + GTP_c
Reaction 51: C51 : oxQ_m + carbamoyl-phosphate_c + L-aspartate ==> H2O + phosphate_c + redQ_m + orotate_c

Reaction 52: C52 : H+_c + 5-phospho-a-D-ribose-1-diphosphate_c + orotate_c ==> CO2_c + diphosphate_c + uridine-5'-phosphate_c
Reaction 53: C53 : ATP_c + uridine-5'-phosphate_c ==> ADP_c + UDP_c
Reaction 54: C54 : ATP_c + UDP_c ==> ADP_c + UTP_c
Reaction 55: C55 : H2O + ATP_c + L-glutamine + UTP_c ==> L-glutamate + 2 H+_c + ADP_c + phosphate_c + CTP_c
Reaction 56: C56 : ATP_c + CTP_c + redthioredoxin_c ==> H+_c + ADP_c + phosphate_c + dCTP_c + oxthioredoxin_c
Reaction 57: C57 : 5,10-methylenetetrahydrofolate_c + 2 ATP_c + UDP_c + redthioredoxin_c ==> H+_c + 2 ADP_c + phosphate_c + dTTP_c + oxthioredoxin_c + 7,8-dihydrofolate-monoglutamate_c
Reaction 58: C58 : H2O + diphosphate_c ==> H+_c + 2 phosphate_c
Reaction 59: C59 : 10 H2O + 2.3 ATP_c + 2.7 GTP_c + 2.3 UTP_c + 2.7 CTP_c ==> 10 H+_c + 10 diphosphate_c + RNA
Reaction 60: C60 : 10 H2O + 2.3 dATP_c + 2.3 dTTP_c + 2.7 dCTP_c + 2.7 dGTP_c ==> 10 H+_c + 10 diphosphate_c + DNA
Reaction 61: C61 : NADPH_c + H+_c + oxthioredoxin_c ==> NADP+_c + redthioredoxin_c
Reaction 62: C62 : NADPH_c + H+_c + 7,8-dihydrofolate-monoglutamate_c ==> NADP+_c + tetrahydrofolate_c
Reaction 63: C63 : L-glutamate + oxaloacetate_c ==> 2-oxoglutarate_c + L-aspartate
Reaction 64: C64 : 4-amino-4-deoxychorismate ==> pyruvate_c + H+_c + p-aminobenzoate_c
Reaction 65: C65 : 3 H2O + ATP_c + GTP_c ==> 3 H+_c + phosphate_c + formate_c + diphosphate_c + AMP_c + glycoaldehyde_c + 6-hydroxymethyl-dihydropterin-diphosphate_c
Reaction 66: C66 : L-glutamate + ATP_c + p-aminobenzoate_c + 6-hydroxymethyl-dihydropterin-diphosphate_c ==> H+_c + ADP_c + phosphate_c + diphosphate_c + 7,8-dihydrofolate-monoglutamate_c
Reaction 67: C67 : ATP_c + acetate_c <==> ADP_c + acetylphosphate_c
Reaction 68: C68 : 5-methyl-tetrahydrofolate_c + acetyl-CoA_c + L-homoserine + hydrogen-sulfide_c ==> H+_c + tetrahydrofolate_c + acetate_c + coenzymeA_c + L-methionine
Reaction 69: C69 : L-serine + acetyl-CoA_c + hydrogen-sulfide_c ==> H+_c + acetate_c + coenzymeA_c + L-cysteine
Reaction 70: C70 : H2O + NADP+_c + D-glyceraldehyde-3-phosphate_c ==> NADPH_c + 2 H+_c + 3-phospho-D-glycerate_c
Reaction 71: C71 : ATP_c + L-homoserine ==> H+_c + ADP_c + O-phospho-L-homoserine
Reaction 72: C72 : H2O + O-phospho-L-homoserine ==> phosphate_c + L-threonine
Reaction 73: C73 : ATP_c + L-aspartate ==> ADP_c + L-aspartyl-4-phosphate_c
Reaction 74: C74 : NADP+_c + phosphate_c + L-aspartate-semialdehyde_c <==> NADPH_c + H+_c + L-aspartyl-4-phosphate_c
Reaction 75: C75 : NADPH_c + H+_c + L-aspartate-semialdehyde_c ==> NADP+_c + L-homoserine
Reaction 76: C76 : 2 pyruvate_c + H+_c ==> CO2_c + (S)-2-acetolactate_c
Reaction 77: C77 : NAD+_c + (R)-lactate_c <==> NADH_c + pyruvate_c + H+_c
Reaction 78: C78 : L-glutamate + H+_c + chorismate ==> H2O + 2-oxoglutarate_c + CO2_c + L-phenylalanine
Reaction 79: C79 : L-serine + L-glutamine + 5-phospho-a-D-ribose-1-diphosphate_c + chorismate ==> 2 H2O + pyruvate_c + L-glutamate + CO2_c + D-glyceraldehyde-3-phosphate_c + diphosphate_c + L-tryptophan
Reaction 80: C80 : H2O + ATP_c + L-glutamine + L-aspartate ==> L-glutamate + H+_c + diphosphate_c + AMP_c + L-asparagine
Reaction 81: C81 : ATP_c + L-aspartate + L-citrulline ==> H+_c + diphosphate_c + AMP_c + L-arginino-succinate_c
Reaction 82: C82 : L-arginino-succinate_c ==> fumarate_c + L-arginine
Reaction 83: C83 : H2O + L-arginine ==> urea_c + L-ornithine
Reaction 84: C84 : L-ornithine ==> ammonia_c + H+_c + L-proline
Reaction 85: C85 : NADH_c + H+_c + dihydroxyacetone-phosphate_c <==> NAD+_c + sn-glycerol-3-phosphate_c
Reaction 86: C86 : sn-glycerol-3-phosphate_c + fattyacid_18_1-CoA_c ==> coenzymeA_c + 1-acyl-sn-glycerol-3-phosphate_c
Reaction 87: C87 : fattyacid_16_0-CoA_c + 1-acyl-sn-glycerol-3-phosphate_c ==> coenzymeA_c + 1,2-diacylglycerol-3-phosphate_c
Reaction 88: C88 : H2O + 1,2-diacylglycerol-3-phosphate_c ==> phosphate_c + 1,2-diacylglycerol_c
Reaction 89: C89 : 1,2-diacylglycerol_c + fattyacid_18_1-CoA_c ==> coenzymeA_c + triacylglycerol_c
Reaction 90: C90 : ATP_c + coenzymeA_c + fattyacid_16_0_c ==> diphosphate_c + AMP_c + fattyacid_16_0-CoA_c
Reaction 91: C91 : 2 H2O + 5-methyl-tetrahydrofolate_c + ATP_c + S-adenosyl-L-homocysteine_c ==> tetrahydrofolate_c + phosphate_c + diphosphate_c + adenosine_c + S-adenosyl-L-methionine_c
Reaction 92: C92 : ATP_c + adenosine_c ==> H+_c + ADP_c + AMP_c
Reaction 93: C93 : ATP_c + coenzymeA_c + fattyacid_18_1_c ==> diphosphate_c + AMP_c + fattyacid_18_1-CoA_c
Reaction 94: C94 : H2O + D-sedoheptulose-1,7-bisphosphate_c ==> phosphate_c + D-sedoheptulose-7-phosphate_c
Reaction 95: C95 : dihydroxyacetone-phosphate_c + D-erythrose-4-phosphate_c <==> D-sedoheptulose-1,7-bisphosphate_c
Reaction 96: C96 : (S)-methylmalonyl-CoA_c <==> succinyl-CoA_c
Reaction 97: C97 : 47 silica + 2 iron + 5 calcium + 35 chloride + 7 magnesium + 5 potasium + zinc ==> ash_biomass
Reaction 98: C98 : 24 H2O + 5 a-D-glucose-6-phosphate_c + 2 D-xylulose-5-phosphate_c + D-ribose-5-phosphate_c + 3 a-D-galactose-1-phosphate_c + 13 D-mannose-6-phosphate_c ==> 24 H+_c + 24 phosphate_c + polysaccharide
Reaction 99: C99 : D-mannose-6-phosphate_c <==> D-fructose-6-phosphate_c
Reaction 100: C100 : H2O + ATP_c + chrysolaminaran_ext ==> H+_c + ADP_c + a-D-glucose-6-phosphate_c
Reaction 101: C101 : H2O + NAD+_c + 2 oxCytoC_m + a-D-galactose-1-phosphate_c ==> NADH_c + 2 H+_c + phosphate_c + 2 redCytoC_m + L-ascorbate
Reaction 102: C102 : 2 D-ribulose-5-phosphate_c + 5-amino-6-(D-ribitylamino)uracil ==> 4 H2O + 3 H+_c + 2 phosphate_c + 2 formate_c + riboflavin
Reaction 103: C103 : NAD+_c + glycine + NADPH_c + L-cysteine ==> 2 H2O + L-alanine + NADP+_c + 2 H+_c + CO2_c + AMP_c + nicotinamide + 4-methyl-5-(2-phosphonooxyethyl)thiazole
Reaction 104: C104 : H2O + glycine + ATP_c + 10-formyl-tetrahydrofolate_c + L-glutamine + 5-phospho-a-D-ribose-1-diphosphate_c ==> L-glutamate + 2 H+_c + tetrahydrofolate_c + ADP_c + phosphate_c + diphosphate_c + 5'-phosphoribosyl-N-formylglycineamide
Reaction 105: C105 : H2O + 2 ATP_c + L-glutamine + 5'-phosphoribosyl-N-formylglycineamide ==> L-glutamate + 2 H+_c + 2 ADP_c + 2 phosphate_c + 5-amino-1-(5-phospho-D-ribosyl)imidazole
Reaction 106: C106 : ATP_c + S-adenosyl-L-methionine_c + 5-amino-1-(5-phospho-D-ribosyl)imidazole ==> 3 H+_c + ADP_c + formate_c + L-methionine + 5'-deoxyadenosine_c + 4-amino-2-methyl-5-diphosphomethylpyrimidine + carbon-monoxide_c
Reaction 107: C107 : 3 ATP_c + 5'-deoxyadenosine_c ==> H+_c + 3 ADP_c + dATP_c

Reaction 108: C108 : H2O + H+_c + 4-methyl-5-(2-phosphonooxyethyl)thiazole + 4-amino-2-methyl-5-diphosphomethylpyrimidine ==> phosphate_c + diphosphate_c + thiamin
Reaction 109: C109 : H2O + ATP_c + L-methionine ==> phosphate_c + diphosphate_c + S-adenosyl-L-methionine_c
Reaction 110: C110 : 5 H2O + NADPH_c + GTP_c ==> NADP+_c + ammonia_c + H+_c + phosphate_c + formate_c + diphosphate_c + 5-amino-6-(D-ribitylamino)uracil
Reaction 111: C111 : H+_c + oxygen_c + dihydroxyacetone-phosphate_c + 5-phospho-a-D-ribose-1-diphosphate_c + L-aspartate ==> 2 H2O + CO2_c + phosphate_c + diphosphate_c + hydrogenperoxide_c + nicotinate-D-ribonucleotide
Reaction 112: C112 : H2O + 2 ATP_c + L-glutamine + nicotinate-D-ribonucleotide ==> NAD+_c + L-glutamate + 2 diphosphate_c + AMP_c
Reaction 113: C113 : 2 H2O + NAD+_c ==> 3 H+_c + AMP_c + D-ribose-5-phosphate_c + nicotinamide
Reaction 114: C114 : 297 H2O + 8.5 L-alanine + 6.4 glycine + 6.1 L-glutamate + 99 ATP_c + 8.4 L-serine + 4.1 L-glutamine + 198 GTP_c + 2.5 L-histidine + 5.9 L-aspartate + 3.8 L-asparagine + 2.3 L-methionine + 1.6 L-cysteine + 4.6 L-lysine + 9.4 L-leucine + 2.6 L-tyrosine + 6.1 L-threonine + 3.7 L-phenylalanine + 1.4 L-tryptophan + 6.2 L-arginine + 5.2 L-proline + 6.8 L-valine + 4.5 L-isoleucine ==> 297 H+_c + 198 phosphate_c + 99 diphosphate_c + 99 AMP_c + 198 GDP_c + protein
Reaction 115: M1 : 3-phospho-L-serine_m + 2-oxoglutarate_m <==> 3-phospho-hydroxypyruvate_m + L-glutamate
Reaction 116: M2 : 2-oxoglutarate_m + L-ornithine ==> L-glutamate + L-glutamate-g-semialdehyde
Reaction 117: M3 : 3-phospho-D-glycerate_m + NAD+_m <==> 3-phospho-hydroxypyruvate_m + NADH_m + H+_m
Reaction 118: M4 : NAD+_m + glycine + tetrahydrofolate_m ==> NADH_m + H+_m + CO2_m + ammonia_m + 5,10-methylenetetrahydrofolate_m
Reaction 119: M5 : NAD+_m + 5,10-methylenetetrahydrofolate_m <==> NADH_m + 5,10-methenyltetrahydrofolate_m
Reaction 120: M6 : L-serine + tetrahydrofolate_m <==> H2O + glycine + 5,10-methylenetetrahydrofolate_m
Reaction 121: M7 : H+_m + phosphoenolpyruvate_m + ADP_m ==> pyruvate_m + ATP_m
Reaction 122: M8 : NAD+_m + pyruvate_m + coenzymeA_m ==> NADH_m + CO2_m + acetyl-CoA_m
Reaction 123: M9 : H2O + acetyl-CoA_m + oxaloacetate_m ==> H+_m + coenzymeA_m + citrate_m
Reaction 124: M10 : citrate_m <==> D-threo-isocitrate_m
Reaction 125: M11 : D-threo-isocitrate_m + NADP+_m ==> 2-oxoglutarate_m + CO2_m + NADPH_m
Reaction 126: M12 : 2-oxoglutarate_m + NAD+_m + coenzymeA_m ==> NADH_m + CO2_m + succinyl-CoA_m
Reaction 127: M13 : succinyl-CoA_m + ADP_m + phosphate_m ==> coenzymeA_m + succinate_m + ATP_m
Reaction 128: M14 : succinate_m + oxQ_m <==> fumarate_m + redQ_m
Reaction 129: M15 : (S)-malate_m <==> H2O + fumarate_m
Reaction 130: M16 : H2O + CO2_m + ammonia_m + 2 ATP_m ==> 2 H+_m + 2 ADP_m + phosphate_m + carbamoyl-phosphate_m
Reaction 131: M17 : H2O + 3-phospho-L-serine_m ==> L-serine + phosphate_m
Reaction 132: M18 : 3-phospho-D-glycerate_m + ATP_m <==> ADP_m + 1,3-diphosphateglycerate_m
Reaction 133: M19 : NAD+_m + phosphate_m + D-glyceraldehyde-3-phosphate_m <==> NADH_m + H+_m + 1,3-diphosphateglycerate_m
Reaction 134: M20 : 3-phospho-D-glycerate_m <==> 2-phospho-D-glycerate_m
Reaction 135: M21 : 2-phospho-D-glycerate_m <==> H2O + phosphoenolpyruvate_m
Reaction 136: M22 : 4 H+_m + redQ_m + 2 oxCytoC_m ==> oxQ_m + 2 redCytoC_m + 4 pmf_m
Reaction 137: M23 : 4 H+_m + oxygen_m + 4 redCytoC_m ==> 2 H2O + 4 oxCytoC_m + 4 pmf_m
Reaction 138: M24 : ADP_m + phosphate_m + 4 pmf_m ==> H2O + 3 H+_m + ATP_m
Reaction 139: M25 : NADH_m + H+_m + oxQ_m ==> NAD+_m + redQ_m
Reaction 140: M26 : NADH_m + 5 H+_m + oxQ_m ==> NAD+_m + redQ_m + 4 pmf_m
Reaction 141: M27 : NAD+_m + NADPH_m + pmf_m ==> NADH_m + H+_m + NADP+_m
Reaction 142: M28 : NADH_m + NADP+_m + pmf_m ==> NAD+_m + H+_m + NADPH_m
Reaction 143: M29 : bicarbonate_m + pyruvate_m + ATP_m ==> H+_m + oxaloacetate_m + ADP_m + phosphate_m
Reaction 144: M30 : oxaloacetate_m + ATP_m ==> CO2_m + phosphoenolpyruvate_m + ADP_m
Reaction 145: M31 : H2O + CO2_m + phosphoenolpyruvate_m ==> H+_m + oxaloacetate_m + phosphate_m
Reaction 146: M32 : NAD+_m + (S)-malate_m ==> NADH_m + CO2_m + pyruvate_m
Reaction 147: M33 : L-ornithine + carbamoyl-phosphate_m ==> H+_m + phosphate_m + L-citrulline
Reaction 148: M34 : H2O + urea_m ==> CO2_m + 2 ammonia_m
Reaction 149: M35 : D-glyceraldehyde-3-phosphate_m <==> dihydroxyacetone-phosphate_m
Reaction 150: M36 : NADH_m + H+_m + hydroxypyruvate_m <==> NAD+_m + D-glycerate_m
Reaction 151: M37 : L-serine + pyruvate_m <==> L-alanine + hydroxypyruvate_m
Reaction 152: M38 : NAD+_m + (S)-lactate_m ==> NADH_m + H+_m + pyruvate_m
Reaction 153: M39 : H2O + 5,10-methenyltetrahydrofolate_m <==> H+_m + 10-formyl-tetrahydrofolate_m
Reaction 154: M40 : 2 H2O + NADP+_m + ATP_m + L-glutamate-g-semialdehyde ==> 3 H+_m + L-glutamate + NADPH_m + ADP_m + phosphate_m
Reaction 155: M41 : L-threonine ==> H+_m + ammonia_m + 2-oxobutanoate
Reaction 156: M42 : H+_m + NADPH_m + 7,8-dihydrofolate-monoglutamate_m ==> tetrahydrofolate_m + NADP+_m
Reaction 157: M43 : NADH_m + H+_m + acetaldehyde_m <==> NAD+_m + ethanol_m
Reaction 158: M44 : H2O + NAD+_m + glycoaldehyde_m ==> NADH_m + 2 H+_m + glycolate_m
Reaction 159: M45 : H2O + NAD+_m + acetaldehyde_m <==> NADH_m + 2 H+_m + acetate_m
Reaction 160: M46 : ATP_m + AMP_m ==> 2 ADP_m
Reaction 161: M47 : H2O + CO2_m <==> H+_m + bicarbonate_m
Reaction 162: M48 : a-D-glucose-6-phosphate_m <==> D-fructose-6-phosphate_m
Reaction 163: M49 : NAD+_m + (S)-malate_m <==> NADH_m + H+_m + oxaloacetate_m
Reaction 164: M50 : bicarbonate_m + acetyl-CoA_m + ATP_m ==> H+_m + ADP_m + phosphate_m + malonyl-CoA_m
Reaction 165: M51 : 6-phospho-D-gluconate_m ==> H2O + 2-dehydro-3-deoxy-D-gluconate-6-phosphate_m
Reaction 166: M52 : 2-dehydro-3-deoxy-D-gluconate-6-phosphate_m ==> pyruvate_m + D-glyceraldehyde-3-phosphate_m
Reaction 167: P1 : D-ribulose-1,5-bisphosphate_p + CO2_p + H2O ==> 2 3-phospho-D-glycerate_p + 2 H+_p
Reaction 168: P2 : D-ribulose-1,5-bisphosphate_p + oxygen_p ==> 2-phosphoglycolate_p + 3-phospho-D-glycerate_p + 2 H+_p
Reaction 169: P3 : 2-phosphoglycolate_p + H2O ==> glycolate_p + phosphate_p

Reaction 170: P4 : D-ribose-5-phosphate_p <==> D-ribulose-5-phosphate_p
Reaction 171: P5 : D-ribulose-5-phosphate_p <==> D-xylulose-5-phosphate_p
Reaction 172: P6 : D-sedoheptulose-7-phosphate_p + D-glyceraldehyde-3-phosphate_p <==> D-ribose-5-phosphate_p + D-xylulose-5-phosphate_p
Reaction 173: P7 : D-xylulose-5-phosphate_p + D-erythrose-4-phosphate_p <==> D-glyceraldehyde-3-phosphate_p + D-fructose-6-phosphate_p
Reaction 174: P8 : D-sedoheptulose-7-phosphate_p + D-glyceraldehyde-3-phosphate_p <==> D-erythrose-4-phosphate_p + D-fructose-6-phosphate_p
Reaction 175: P9 : H2O + fructose-1,6-bisphosphate_p ==> phosphate_p + D-fructose-6-phosphate_p
Reaction 176: P10 : D-fructose-6-phosphate_p + ATP_p <==> H+_p + fructose-1,6-bisphosphate_p + ADP_p
Reaction 177: P11 : fructose-1,6-bisphosphate_p <==> D-glyceraldehyde-3-phosphate_p + dihydroxyacetone-phosphate_p
Reaction 178: P12 : D-glyceraldehyde-3-phosphate_p <==> dihydroxyacetone-phosphate_p
Reaction 179: P13 : phosphate_p + D-glyceraldehyde-3-phosphate_p + NADP+_p <==> H+_p + 1,3-diphosphateglycerate_p + NADPH_p
Reaction 180: P14 : 3-phospho-D-glycerate_p + ATP_p <==> ADP_p + 1,3-diphosphateglycerate_p
Reaction 181: P15 : 3-phospho-D-glycerate_p <==> 2-phospho-D-glycerate_p
Reaction 182: P16 : 2-phospho-D-glycerate_p <==> H2O + phosphoenolpyruvate_p
Reaction 183: P17 : D-ribulose-5-phosphate_p + ATP_p ==> D-ribulose-1,5-bisphosphate_p + H+_p + ADP_p
Reaction 184: P18 : NADP+_p + tetrahydrofolate_p ==> H+_p + NADPH_p + 7,8-dihydrofolate-monoglutamate_p
Reaction 185: P19 : 7 H+_p + nitrite_p + 6 redferredoxin_p ==> 2 H2O + ammonia_p + 6 oxferredoxin_p
Reaction 186: P20 : oxferredoxin_p + hv_p + redPC_p ==> redferredoxin_p + oxPC_p
Reaction 187: P21 : H+_p + 2 redferredoxin_p + NADP+_p ==> 2 oxferredoxin_p + NADPH_p
Reaction 188: P22 : 4 H+_p + 2 redferredoxin_p + oxPQ_p ==> 2 oxferredoxin_p + redPQ_p + 2 pmf_p
Reaction 189: P23 : 4 H+_p + 2 oxPC_p + redPQ_p ==> 2 redPC_p + oxPQ_p + 6 pmf_p
Reaction 190: P24 : 4 H+_p + 2 H2O + 4 hv_p + 2 oxPQ_p ==> oxygen_p + 2 redPQ_p + 4 pmf_p
Reaction 191: P25 : phosphate_p + ADP_p + 4 pmf_p ==> 3 H+_p + H2O + ATP_p
Reaction 192: P26 : 2 H+_p + 2-oxoglutarate_p + 2 redferredoxin_p + L-glutamine ==> 2 L-glutamate + 2 oxferredoxin_p
Reaction 193: P27 : ATP_p + L-glutamate + ammonia_p ==> phosphate_p + ADP_p + L-glutamine
Reaction 194: P28 : CO2_p + H2O <==> H+_p + bicarbonate_p
Reaction 195: P29 : H2O + NAD+_p + acetaldehyde_p <==> 2 H+_p + NADH_p + acetate_p
Reaction 196: P30 : NAD+_p + ethanol_p <==> H+_p + NADH_p + acetaldehyde_p
Reaction 197: P31 : ATP_p + acetate_p + coenzymeA_p ==> acetyl-CoA_p + diphosphate_p + AMP_p
Reaction 198: P32 : ATP_p + bicarbonate_p + pyruvate_p ==> H+_p + phosphate_p + ADP_p + oxaloacetate_p
Reaction 199: P33 : H+_p + ADP_p + phosphoenolpyruvate_p ==> ATP_p + pyruvate_p
Reaction 200: P34 : phosphate_p + ATP_p + pyruvate_p ==> H+_p + phosphoenolpyruvate_p + diphosphate_p + AMP_p
Reaction 201: P35 : NAD+_p + NADPH_p + pmf_p ==> H+_p + NADH_p + NADP+_p
Reaction 202: P36 : NADH_p + NADP+_p + pmf_p ==> H+_p + NAD+_p + NADPH_p
Reaction 203: P37 : L-glutamine + chorismate ==> L-glutamate + 4-amino-4-deoxychorismate
Reaction 204: P38 : chorismate <==> prephenate
Reaction 205: P39 : H+_p + 2 pyruvate_p <==> CO2_p + (S)-2-acetolactate_p
Reaction 206: P40 : 2 H+_p + pyruvate_c + L-glutamate + NADPH_c + L-aspartate-semialdehyde_c ==> CO2_p + H2O + 2-oxoglutarate_p + NADP+_c + L-lysine
Reaction 207: P41 : D-erythrose-4-phosphate_p + ATP_p + 2 phosphoenolpyruvate_p + NADPH_p ==> 4 phosphate_p + ADP_p + NADP+_p + chorismate
Reaction 208: P42 : NAD+_p + L-glutamate + NADPH_p + acetyl-CoA_p + (S)-2-acetolactate_p ==> CO2_p + NADH_p + 2-oxoglutarate_p + NADP+_p + coenzymeA_p + L-leucine
Reaction 209: P43 : L-glutamate + NADP+_p + prephenate ==> CO2_p + 2-oxoglutarate_p + NADPH_p + L-tyrosine
Reaction 210: P44 : 2 H+_p + L-glutamate + NADPH_p + pyruvate_p + 2-oxobutanoate ==> CO2_p + H2O + 2-oxoglutarate_p + NADP+_p + L-isoleucine
Reaction 211: P45 : 2 H+_p + L-glutamate + NADPH_p + 2 pyruvate_p ==> CO2_p + H2O + 2-oxoglutarate_p + NADP+_p + L-valine
Reaction 212: P46 : ATP_p + AMP_p ==> 2 ADP_p
Reaction 213: P47 : 2 H+_p + H2O + diphosphate_p ==> 2 phosphate_p + 3 pmf_p
Reaction 214: P48 : 6 H+_p + 6 redferredoxin_p + 2 ATP_c + redthioredoxin_p + sulfate_c ==> 2 H2O + phosphate_p + 6 oxferredoxin_p + ADP_c + diphosphate_c + AMP_c + oxthioredoxin_p + hydrogen-sulfide_p
Reaction 215: P49 : H+_p + NADPH_p + oxthioredoxin_p ==> NADP+_p + redthioredoxin_p
Reaction 216: P50 : H+_p + H2O + ATP_p + 2 L-glutamate + NADPH_p + acetyl-CoA_c ==> phosphate_p + ADP_p + H+_m + 2-oxoglutarate_p + NADP+_p + coenzymeA_c + acetate_p + L-ornithine
Reaction 217: P51 : acetyl-CoA_p + holo-[acp]_p ==> coenzymeA_p + acetyl-[acp]_p
Reaction 218: P52 : ATP_p + bicarbonate_p + acetyl-CoA_p ==> H+_p + phosphate_p + ADP_p + malonyl-CoA_p
Reaction 219: P53 : H+_p + holo-[acp]_p + malonyl-CoA_p ==> coenzymeA_p + malonyl-[acp]_p
Reaction 220: P54 : H+_p + NADPH_p + acetoacetyl-[acp]_p ==> NADP+_p + (R)-3-hydroxybutanoyl-[acp]_p
Reaction 221: P55 : H+_p + NADH_p + (R)-3-hydroxybutanoyl-[acp]_p ==> H2O + NAD+_p + butyryl-[acp]_p
Reaction 222: P56 : 12 H+_p + 6 NADH_p + 6 NADPH_p + 6 malonyl-[acp]_p + butyryl-[acp]_p ==> 6 CO2_p + 6 H2O + 6 NAD+_p + 6 NADP+_p + 6 holo-[acp]_p + fattyacid_16_0_[acp]_p
Reaction 223: P57 : malonyl-[acp]_p + acetyl-[acp]_p ==> CO2_p + holo-[acp]_p + acetoacetyl-[acp]_p
Reaction 224: P58 : H2O + 6-phospho-D-glucono-1,5-lactone_p <==> H+_p + 6-phospho-D-gluconate_p
Reaction 225: P59 : 8 ATP_p + 8 L-glutamate + 8 NADPH_p ==> 8 H2O + 4 ammonia_p + 8 NADP+_p + 8 diphosphate_p + 8 AMP_p + uroporphyrinogen-III_p
Reaction 226: P60 : 7 oxygen_p + 8 H+_p + ATP_p + 5 NADPH_p + uroporphyrinogen-III_p + S-adenosyl-L-methionine_p ==> 6 CO2_p + 6 H2O + phosphate_p + ADP_p + 5 NADP+_p + S-adenosyl-L-homocysteine_p + 3 hydrogenperoxide_p + chlorophyllide-a_p

Reaction 227: P61 : 4 H+_p + 3 NADPH_p + chlorophyllide-a_p + all-trans-geranyl-geranyl-diphosphate_p ==> 3 NADP+_p + diphosphate_p + chlorophyll-a
Reaction 228: P62 : 3 H+_p + D-glyceraldehyde-3-phosphate_p + ATP_p + 2 redferredoxin_p + NADPH_p + pyruvate_p + CTP_p ==> CO2_p + H2O + ADP_p + 2 oxferredoxin_p + NADP+_p + diphosphate_p + CMP_p + 1-hydroxy-2-methyl-2-(E)-butenyl-4-diphosphate_p
Reaction 229: P63 : 4 H+_p + 4 NADPH_p + 4 1-hydroxy-2-methyl-2-(E)-butenyl-4-diphosphate_p ==> 4 H2O + 4 NADP+_p + 3 diphosphate_p + all-trans-geranyl-geranyl-diphosphate_p
Reaction 230: P64 : oxygen_p + 3 H+_p + NADH_p + 2 NADPH_p + malonyl-[acp]_p + fattyacid_16_0_[acp]_p ==> CO2_p + 3 H2O + NAD+_p + 2 NADP+_p + holo-[acp]_p + fattyacid_18_1_[acp]_p
Reaction 231: P65 : 2 ATP_p + CMP_p ==> 2 ADP_p + CTP_p
Reaction 232: P66 : a-D-glucose-1-phosphate_p <==> a-D-glucose-6-phosphate_p
Reaction 233: P67 : a-D-glucose-6-phosphate_p <==> D-fructose-6-phosphate_p
Reaction 234: P68 : D-erythrose-4-phosphate_p + dihydroxyacetone-phosphate_p <==> D-sedoheptulose-1,7-bisphosphate_p
Reaction 235: P69 : 4 oxygen_p + 4 H+_p + 2 NADH_p + 2 NADPH_p + 4 oxPQ_p + 2 all-trans-geranyl-geranyl-diphosphate_p ==> 4 H2O + 2 NAD+_p + 2 NADP+_p + 4 redPQ_p + 2 diphosphate_p + violaxanthin
Reaction 236: P70 : 3 H+_p + 3 NADPH_p + all-trans-geranyl-geranyl-diphosphate_p ==> 3 NADP+_p + phytyl-diphosphate_p
Reaction 237: P71 : 2-oxoglutarate_p + L-tyrosine ==> L-glutamate + 4-hydroxyphenylpyruvate_p
Reaction 238: P72 : oxygen_p + 2 S-adenosyl-L-methionine_p + phytyl-diphosphate_p + 4-hydroxyphenylpyruvate_p ==> H+_p + 2 CO2_p + diphosphate_p + 2 S-adenosyl-L-homocysteine_p + a-tocopherol
Reaction 239: P73 : ==>
Reaction 240: P74 : 2 H+_p + 2 superoxide_p ==> oxygen_p + hydrogenperoxide_p
Reaction 241: P75 : H+_p + NADPH_p + hydrogenperoxide_p ==> 2 H2O + NADP+_p
Reaction 242: T1 : nitrate_ext ==> nitrate_c
Reaction 243: T2 : nitrite_c ==> nitrite_p
Reaction 244: T3 : ammonia_p ==> ammonia_c
Reaction 245: T4 : CO2_c ==> CO2_ext
Reaction 246: T5 : CO2_c <==> CO2_m
Reaction 247: T6 : CO2_c <==> CO2_p
Reaction 248: T7 : CO2_c <==> CO2_x
Reaction 249: T8 : bicarbonate_ext ==> bicarbonate_c
Reaction 250: T9 : bicarbonate_c <==> bicarbonate_m
Reaction 251: T10 : bicarbonate_c <==> bicarbonate_p
Reaction 252: T11 : bicarbonate_c <==> bicarbonate_x
Reaction 253: T12 : ammonia_m <==> ammonia_c
Reaction 254: T13 : carbamoyl-phosphate_m <==> carbamoyl-phosphate_c
Reaction 255: T14 : silica_ext ==> silica
Reaction 256: T15 : H2O + ATP_c + calcium_ext ==> H+_c + ADP_c + phosphate_c + calcium
Reaction 257: T16 : H2O + ATP_c + potasium_ext ==> H+_c + ADP_c + phosphate_c + potasium
Reaction 258: T17 : ADP_c + phosphate_c + ATP_m <==> ATP_c + ADP_m + phosphate_m
Reaction 259: T18 : ATP_p + phosphate_c + ADP_ps <==> phosphate_p + ADP_p + ATP_ps
Reaction 260: T19 : glycolate_p ==> glycolate_c
Reaction 261: T20 : glycolate_c ==> glycolate_x
Reaction 262: T21 : glyoxylate_c <==> glyoxylate_m
Reaction 263: T22 : glyoxylate_x ==> glyoxylate_c
Reaction 264: T23 : H2O + ATP_c + iron_ext ==> H+_c + ADP_c + phosphate_c + iron
Reaction 265: T24 : acetyl-CoA_c + coenzymeA_p ==> coenzymeA_c + acetyl-CoA_p
Reaction 266: T25 : pyruvate_c ==> pyruvate_m
Reaction 267: T26 : oxygen_p <==> oxygen_c
Reaction 268: T27 : oxygen_c <==> oxygen_m
Reaction 269: T28 : oxygen_c <==> oxygen_x
Reaction 270: T29 : oxygen_ext <==> oxygen_c
Reaction 271: T30 : 2-oxoglutarate_c + phosphate_m <==> 2-oxoglutarate_m + phosphate_c
Reaction 272: T31 : phosphate_ext <==> phosphate_c
Reaction 273: T32 : ammonia_c ==> ammonia_ext
Reaction 274: T33 : glyoxylate_c ==> glyoxylate_p
Reaction 275: T34 : H+_m + phosphate_c + citrate_m <==> H+_c + phosphate_m + citrate_c
Reaction 276: T35 : D-glyceraldehyde-3-phosphate_p + phosphate_c ==> phosphate_p + D-glyceraldehyde-3-phosphate_c
Reaction 277: T36 : phosphoenolpyruvate_p + phosphate_c ==> phosphate_p + phosphoenolpyruvate_c
Reaction 278: T37 : phosphate_p + 3-phospho-D-glycerate_c <==> 3-phospho-D-glycerate_p + phosphate_c
Reaction 279: T38 : H+_c + phosphate_c <==> H+_m + phosphate_m
Reaction 280: T39 : H+_c + phosphate_c <==> H+_p + phosphate_p
Reaction 281: T40 : acetyl-CoA_c + CoenzymeA_x <==> coenzymeA_c + acetyl-CoA_x
Reaction 282: T41 : phosphate_p + D-xylulose-5-phosphate_c ==> D-xylulose-5-phosphate_p + phosphate_c
Reaction 283: T42 : urea_c ==> urea_m
Reaction 284: T43 : phosphate_m + fumarate_c <==> phosphate_c + fumarate_m
Reaction 285: T44 : sulfate_ext ==> sulfate_c
Reaction 286: T45 : hydrogen-sulfide_p ==> hydrogen-sulfide_c
Reaction 287: T46 : hv_ext ==> hv_p
Reaction 288: T47 : phosphate_c + (S)-malate_m <==> phosphate_m + (S)-malate_c
Reaction 289: T48 : phosphate_m + oxaloacetate_c <==> phosphate_c + oxaloacetate_m
Reaction 290: T49 : phosphate_m + succinate_c <==> phosphate_c + succinate_m

Reaction 291: T50 : S-adenosyl-L-homocysteine_p + S-adenosyl-L-methionine_c <==> S-adenosyl-L-methionine_p + S-adenosyl-L-homocysteine_c
Reaction 292: T51 : coenzymeA_m + acetyl-CoA_c <==> acetyl-CoA_m + coenzymeA_c
Reaction 293: T52 : H2O + fattyacid_16_0_[acp]_p ==> H+_p + holo-[acp]_p + fattyacid_16_0_c
Reaction 294: T53 : hydrogenperoxide_p ==> hydrogenperoxide_x
Reaction 295: T54 : H2O + fattyacid_18_1_[acp]_p ==> H+_p + holo-[acp]_p + fattyacid_18_1_c
Reaction 296: T55 : glycolate_c ==> glycolate_ext
Reaction 297: T56 : phosphate_m + oxaloacetate_c <==> phosphate_c + oxaloacetate_p
Reaction 298: T57 : H+_ext <==> H+_c
Reaction 299: T58 : H+_c <==> H+_m
Reaction 300: T59 : H+_c <==> H+_p
Reaction 301: T60 : H+_c <==> H+_x
Reaction 302: T61 : H2O + ATP_c + magnesium_ext ==> H+_c + ADP_c + phosphate_c + magnesium
Reaction 303: T62 : chloride_ext ==> chloride
Reaction 304: T63 : H2O + ATP_c + zinc_ext ==> H+_c + ADP_c + phosphate_c + zinc
Reaction 305: T64 : phosphate_m + 6-phospho-D-gluconate_c <==> phosphate_c + 6-phospho-D-gluconate_m
Reaction 306: T65 : phosphate_c + a-D-glucose-6-phosphate_p ==> phosphate_p + a-D-glucose-6-phosphate_c
Reaction 307: T66 : succinate_c + fumarate_p <==> fumarate_c + succinate_p
Reaction 308: T67 : phosphate_c + fumarate_p ==> phosphate_p + fumarate_c
Reaction 309: T68 : glycoaldehyde_c <==> glycoaldehyde_m
Reaction 310: T69 : carbon-monoxide_c ==> carbon-monoxide_ext
Reaction 311: T70 : hydrogenperoxide_c ==> hydrogenperoxide_x
Reaction 312: X1 : 2 hydrogenperoxide_x ==> 2 H2O + oxygen_x
Reaction 313: X2 : H2O + glyoxylate_x + acetyl-CoA_x ==> H+_x + (S)-malate_x + CoenzymeA_x
Reaction 314: X3 : NADH_x + H+_x + dihydroxyacetone-phosphate_x ==> NAD+_x + sn-glycerol-3-phosphate_x
Reaction 315: X4 : glycolate_x + oxygen_x ==> glyoxylate_x + hydrogenperoxide_x
Reaction 316: X5 : (S)-malate_x + NADP+_x ==> CO2_x + pyruvate_x + NADPH_x
Reaction 317: X6 : D-threo-isocitrate_x ==> glyoxylate_x + succinate_x
Reaction 318: mainATP_C : H2O + ATP_c ==> H+_c + ADP_c + phosphate_c + ATP_main
Reaction 319: biomass_syn : 617 chrysolaminaran + 35.4 RNA + 9.2 DNA + 32.8 protein + 163.5 1,2-diacylglycerol-3-phosphate_c + 93 triacylglycerol_c + 22.4 chlorophyll-a + 16.6 violaxanthin + 30.2 ash_biomass + 23.6 polysaccharide + 14.3 L-ascorbate + 4.1 nicotinamide + 2.7 thiamin + 0.23 a-tocopherol + 0.27 riboflavin ==> biomass_ext

Reaction Diagram for Task 4 with *Phaeodactylum tricornutum*